

# Bridge indices of spatial graphs and diagram colorings

Sarah Blackwell, Puttipong Pongtanapaisan, and Hanh Vo

October 31, 2024

## Abstract

We extend the Wirtinger number of links, an invariant originally defined by Blair et al. in terms of extending initial colorings of some strands of a diagram to the entire diagram, to spatial graphs. We prove that the Wirtinger number equals the bridge index of spatial graphs, and we implement an algorithm in Python which gives a more efficient way to estimate upper bounds of bridge indices. Combined with lower bounds from diagram colorings by elements from certain algebraic structures, we obtain exact bridge indices for a large family of spatial graphs.

## 1 Introduction

The *bridge index* has been a useful complexity measure of knots and links since the 1950s, when Schubert used it to show that a knot has only finitely many companions [Sch54]. Since then, the bridge index has also been used to estimate several geometric quantities such as distortion [Par11; Bla+20a], lattice stick number [Ada+12], and total curvature [Mil50]. It is conjectured that the bridge index equals an algebraic quantity called the *meridional rank*; a counterexample has not yet been discovered (see Problem 1.11 in Kirby’s list [Kir97]). Blair et al. verified that this conjecture holds for a large family of links by rephrasing the bridge index algorithmically [Bla+20b; BBK21].

Knots and links can be considered as a proper subclass of *spatial graphs*, which encompass embeddings of 1-complexes. These graphs embedded in 3-space are objects of interest to chemists, as atoms of a molecule and their chemical bonds can be modeled as vertices and edges of a spatial graph, respectively [CEH08]. Additionally, conclusions about abstract graphs can be made by considering how they are spatially embedded in space. For example, the complete graphs  $K_6$  and  $K_7$  fall into two distinct levels in a filtration of abstract graphs formed by considering the minimum number of links in any embedding of the graph: any embedding of  $K_6$  (resp.  $K_7$ ) in 3-space contains at least one link (resp. 21 links) [FM09].

Various authors have generalized the bridge index to spatial graphs, and some have shown that their version still approximates curvature as the bridge index of knots does [ST02; GY12]. There are some properties however that do not carry over to the more general setting. For instance, any knot with bridge index exactly two is prime [Sch56], but this is no longer true for  $\Theta$ -graphs [Mot00]. For non-prime spatial graphs, there exist estimates for the bridge indices in terms of the number of summands [TT21].

Since a random spatial graph encountered in nature usually does not have a simple diagram, it is beneficial to generalize the method of [Bla+20b] to systematically compute the bridge indices of spatial graphs from inputs that are computer-friendly. Our procedure can be summarized as follows. Given a spatial graph diagram, we remove vertices of degree at least three to get diagrams with free ends. We then pick a subset of strands to color and define a move that extends a color to an additional strand provided some conditions are met at a crossing. Roughly, the *Wirtinger number* is the minimum number of initial colorings that extend to the entire diagram by the move, minimized over all diagrams (see Section 2.3 for a formal definition). This quantity turns out to equal the bridge index, which we prove in Section 3.

**Theorem 1.1.** *For spatial graphs, the Wirtinger number equals the bridge index.*

We use our main result, which we implement as an algorithm in Python, to provide upper estimates for the bridge index of a variety of spatial graphs. In some cases we combine our techniques with algebraic lower bounds, which we detail in Section 4, to compute exact values. We use our methods to give several short proofs in Section 5 that the bridge index of spatial graphs can be arbitrarily large (see Corollary 5.9, Corollary 5.13, and Corollary 5.18).

**Corollary 1.2.** *The bridge index of a spatial graph can be arbitrarily large.*

Throughout Section 5 we provide many example computations. In particular, spatial graph whose vertices all have degree four can be obtained from link diagrams by turning some crossings into vertices, or fusing maxima and minima. We can compute exact bridge indices for spatial graphs obtained from generalized Montesinos links by fusing some maxima and minima together (see Example 5.17). In some cases, these fusing operations can still produce interesting almost unknotted graphs. Our Python code can be found at <https://github.com/hanhv/graph-wirt>.

## Acknowledgments

Some of this work was conducted when the first author visited the other two at Arizona State University, and she thanks the mathematics department for their hospitality. We would like to thank Julien Paupert for support and helpful advice. SB was supported by the NSF Postdoctoral Research Fellowship DMS-2303143.

## Contents

<b>1</b>	<b>Introduction</b>	<b>1</b>
<b>2</b>	<b>Preliminaries</b>	<b>3</b>
2.1	Spatial graphs . . . . .	3
2.2	Bridge splittings . . . . .	4
2.3	Wirtinger number . . . . .	5
2.4	Braids . . . . .	6

<b>3</b>	<b>Main result</b>	<b>6</b>
<b>4</b>	<b>Lower bounds</b>	<b>12</b>
4.1	Quandle colorings . . . . .	12
4.2	Meridional rank . . . . .	14
<b>5</b>	<b>Computations</b>	<b>15</b>
5.1	Python code . . . . .	16
5.2	Hara's graphs and modifications . . . . .	18
5.3	Families from vertex sums . . . . .	19
5.4	Eulerian spatial graphs from links . . . . .	21

## 2 Preliminaries

### 2.1 Spatial graphs

A *graph*  $G$  is a set  $(V, E)$  of vertices and edges, where  $G = E \subset V \times V$ . A *spatial graph* is an embedding of a graph  $G$  in  $S^3$  taking vertices to points in  $S^3$  and taking edges  $(u, v)$  to an arc whose endpoints are images of  $u$  and  $v$ . We say a spatial graph is *trivial* if it can be isotoped to lie in the plane.

A vertex  $v$  has *degree*  $k$ , or is  *$k$ -valent*, if it is connected to  $k$  edges. In this paper, we do not consider embeddings of graphs with degree one vertices. Topologically, we can isotope the edge adjacent to a degree one vertex freely so that it does not contribute to the knotting. We treat degree two vertices as parts of edges; that is, we consider the two edges connected to the vertex to be the same as if we combined the two edges into one edge without a vertex there.

Two of the most simple types of spatial graphs, which we will encounter throughout the paper, are  $\Theta$ -graphs and *handcuff graphs*. A spatial  $\Theta$ -graph has two vertices  $u$  and  $v$ , with the underlying graph type  $\{(u, v), (u, v), (u, v)\}$ . A spatial handcuff graph also has two vertices, but with the underlying graph type  $\{(u, u), (u, v), (v, v)\}$ . We can generalize the notion of  $\Theta$ -graphs to  $\Theta_n$ -graphs, which have  $n$  edges between the two vertices (for  $n \geq 4$ ).

A straightforward way to construct a spatial graph is to start with a link, and then add some edges. This way, the complexity of the knotted graph is obtained from the original link. This motivates the study of the following class of spatial graphs. A spatial graph is *almost unknotted* if all of its proper subgraphs are trivial. For  $\Theta$ -graphs, this means each *constituent knot*, that is, the knot obtained by deleting one of the three edges, is the unknot.

A common way to construct more complicated spatial graphs is to form composite spatial graphs, analogous to forming composite numbers from prime numbers. Let  $G_1, G_2$  be spatial graphs in  $S^3$ . Consider a point  $p_1 \in G_1$  and another point  $p_2 \in G_2$ . Removing small regular neighborhoods of  $p_1, p_2$  create spherical boundaries that can be identified together. The resulting space is another spatial graph in  $S^3$ . If  $p_1$  and  $p_2$  both lie in the interior of edges, then the resulting graph is a *connected sum* and we denote it by  $G_1 \# G_2$ . When  $p_1$  and  $p_2$  are both vertices of degree  $k$ , then the resulting graph is a  *$k$ -valent vertex sum* and we denote it by  $G_1 \#_k G_2$ .

## 2.2 Bridge splittings

For our definition of bridge splitting, we follow Taylor and Tomova [TT13]. We call a properly embedded graph  $\tau$  in a 3-ball  $B$  a *trivial tangle* if the following two conditions are satisfied:

- (1) each connected component of  $\tau$  is either a *bridge arc*, which is an edge with both endpoints on  $\partial B$ , or a *pod*, which is a graph with a single vertex in the interior of  $B$  and with all degree one vertices contained in  $\partial B$ , and
- (2) all components of  $\tau$  are simultaneously boundary parallel into  $\partial B$ . This means that for each component  $t$  of  $\tau$  there is a disk  $D$  containing  $t$  with  $\partial D$  inessential in  $\partial B$ .

The *degree* of a pod is defined to be the degree of the single vertex in the interior of  $B$ . By convention, we assume pods have degree  $\geq 3$ . (Degree two vertices are treated as parts of bridge arcs.) See Figure 1 for an example of a trivial tangle. We will glue these trivial tangles along these degree one vertices to form closed spatial graphs in  $S^3$ , and in general, we think of the resulting closed spatial graphs as no longer having vertices where we glued.

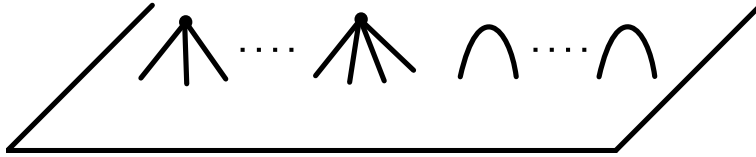


Figure 1: A trivial tangle, where we have displayed pods with degrees two and three, but in general we allow pods of any degrees. We did not include vertices where the tangle intersects  $\partial B$ , since when we glue two trivial tangles together along these vertices, we think of the resulting closed spatial graph as no longer having vertices where we glued.

A *bridge splitting* of a spatial graph  $G$  in the 3-sphere  $S^3$  is a decomposition into two trivial tangles  $(S^3, G) = (B_1, \tau_1) \cup (B_2, \tau_2)$ . We sometimes refer to the pods in  $(B_1, \tau_1)$  as *upper pods* and the pods in  $(B_2, \tau_2)$  as *lower pods*. For bridge splittings of links in  $S^3$ , each tangle has the same number of maxima, and we call the minimum number of maxima over all possible bridge splittings the *bridge index*. Note however that in general the tangles in a bridge splitting of a spatial graph may have a different number of maxima. For this reason there exist multiple definitions of bridge index for spatial graphs in the literature. Our definition will be the following.

**Definition 2.1.** The *bridge index* of a particular bridge splitting  $(S^3, G) = (B_1, \tau_1) \cup (B_2, \tau_2)$  of a spatial graph  $G$  is the minimum number of connected components  $|\tau_1|$ . The *bridge index* of a spatial graph  $G$ , denoted  $\beta(G)$ , is the minimum bridge index over all bridge splittings for  $G$ .

When it is clear from context, we may abuse notation and use  $\beta(G)$  to denote the bridge index of a particular bridge splitting of a graph as well. In the case of  $\Theta_n$ -graphs, the discrepancy around defining the bridge index disappears, as the two trivial tangles in a bridge splitting of a  $\Theta_n$ -graph will always have the same number of maxima, provided that we place one vertex in each tangle.

**Remark 2.2.** When  $G$  is a  $\Theta_n$ -graph and we require that each  $\tau_i$  contains only one vertex of  $G$ , Definition 2.1 reduces to the definitions given in [God97; Mot00; Tsu03].

**Remark 2.3.** Once the number of components of one of the trivial tangles  $|\tau_1|$  is known, one can calculate the number of components of the other trivial tangle  $|\tau_2|$  in a bridge splitting as follows. Let  $\chi(G)$  be the number of vertices of  $G$  minus the number of edges of  $G$ . To keep track of the local maxima, we put a vertex of degree two at each local maximum which is a bridge arc. At the moment, the number of vertices is  $|\tau_1| + |\tau_2|$ . The number of edges can then be determined by examining the sum of the degrees of the vertices in  $\tau_1$ :  $\sum_{1 \leq i \leq |\tau_1|} d_i$ . It follows that

$$\chi(G) = |\tau_1| + |\tau_2| - \sum_{1 \leq i \leq |\tau_1|} d_i.$$

## 2.3 Wirtinger number

Given a spatial graph  $G$  in  $S^3$ , a *diagram*  $D$  for  $G$  is a generic immersion of  $G$  into the plane with each crossing labeled as an overcrossing or an undercrossing. Our new formulation of the bridge index starts with the formation a modified diagram from the original spatial graph diagram.

**Definition 2.4.** Let  $D$  be a diagram for a spatial graph. A *truncated diagram* is the result of removing vertices of degree  $d > 2$  from  $D$ . We refer to the remaining pieces of the graph near removed vertices as *free ends*. A *strand* of a truncated diagram is one of the following:

- (1) an arc connecting an undercrossing to a free end, or
- (2) an arc connecting two undercrossings.

We now describe a process for coloring a truncated diagram. First choose  $k$  distinct colors, and color a subset of strands of  $D$  using these  $k$  colors, where the coloring does not repeat unless a color is assigned to strands that came from removing a degree  $d > 2$  vertex. In the latter case, we use the same color. These  $k$  initial colors are called *seeds*. Sometimes we will also refer to the strands which are colored the initial colors as seeds (where strands coming from the removal of a degree  $d > 2$  vertex count as one seed, as they are all one color).

Then continue to color any uncolored strands using the following *coloring move*, which extends the coloring of a colored arc which passes under another colored arc to the other arc passing under the overstrand. See Figure 2. Note that the coloring move is valid both when the overstrand matches and does not match the color of the understrand; all that matters is that the overstrand has been colored. Also, while strands which came from the removal of a degree  $d > 2$  vertex must be colored the same color if they are included as a seed, such strands in general can end up being colored with different colors if not included as a seed.

If a truncated diagram for a spatial graph can be completely colored by starting with  $k$  seeds and extending these colors using the coloring move, we call the corresponding non-truncated diagram *k-Wirtinger colorable*. See Figure 3 for an example of a 3-Wirtinger colorable diagram for a spatial  $\Theta$ -graph. It is an exercise to check that this diagram is *not* 2-Wirtinger colorable. In fact, our Python code checks for all possible combinations of strands given a fixed number of colors.

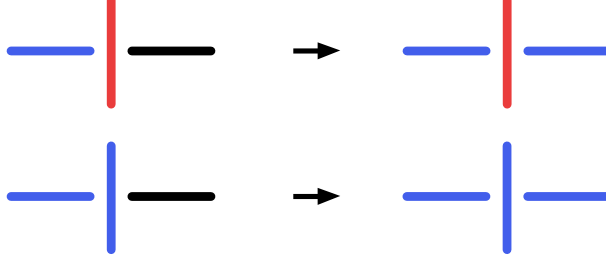


Figure 2: The coloring move: if the overstrand is colored and one of the understrands at the crossing is colored (with possibly the same color), then the move extends the coloring to the other understrand.

In a  $k$ -Wirtinger colored diagram at the final stage, there are certain types of crossings that play an important role in our results. A crossing is called a *multi-colored crossing* if the corresponding understrands received different colors.

We are now ready to define the Wirtinger number of a spatial graph.

**Definition 2.5.** The *Wirtinger number of a spatial graph diagram*  $D$ , denoted  $\omega(D)$ , is the minimal value of  $k$  for which the diagram is  $k$ -Wirtinger colorable; in other words, the smallest number of seeds required to color the entire diagram. The *Wirtinger number of a spatial graph*  $G$ , denoted  $\omega(G)$ , is the minimal Wirtinger number over all diagrams for  $G$ .

**Remark 2.6.** From the proof of our main theorem, we will see that the number  $|\tau_2|$  can also be determined from a  $k$ -Wirtinger colored diagram as the number of multi-colored crossings plus the number of non-seed pods.

## 2.4 Braids

An  $n$ -string braid is a set of  $n$  strings in  $\mathbb{R}^3$  with one endpoint of each string attached to a horizontal plane  $z = b$ , and the other endpoint attached to another horizontal plane  $z = a$ , where  $a < b$ , with the additional requirement that as we move along each string from the top plane to the bottom plane, the string heads downwards and never backtracks. An observation we will frequently use is that as we travel along a spatial graph, we turn around to travel in the opposite direction at the local extrema.

**Observation 2.1.** Suppose that for a bridge-split spatial graph the upper pods and local maxima are at the same level. Suppose also that at a lower height, the lower pods and local minima are at the same level. Then removing small open neighborhoods of the vertices at the pods and the local maxima and minima results in a braid.

## 3 Main result

We phrase our proof in this section in terms of spatial graphs in  $\mathbb{R}^3$  instead of  $S^3 = \mathbb{R}^3 \cup \{\infty\}$ , but this does not make the result less general since the isotopy classes of spatial graphs in  $S^3$  and  $\mathbb{R}^3$  are the same: the point at infinity  $\{\infty\}$  can be taken to be disjoint from a spatial graph and its isotopies.

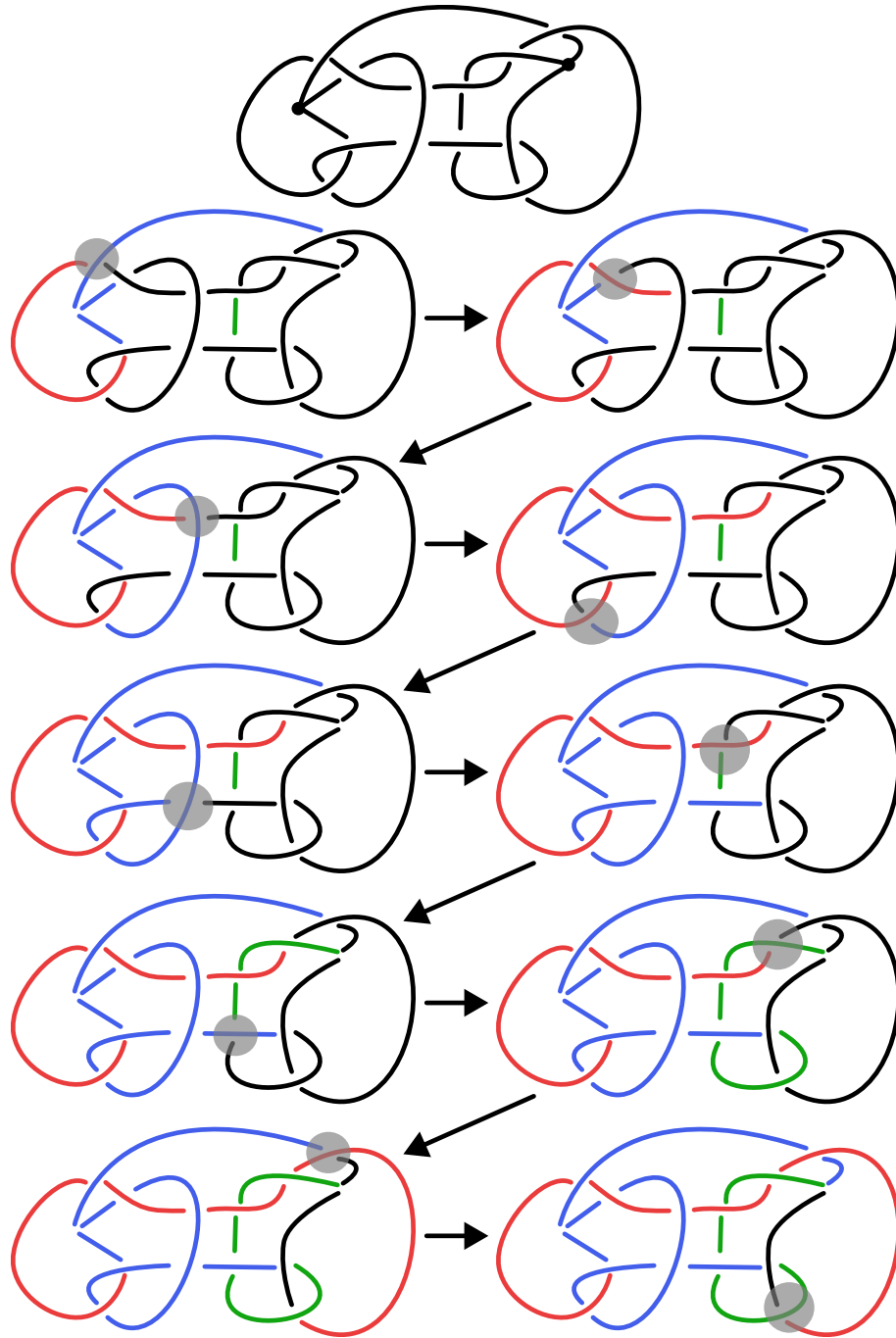


Figure 3: This diagram is 3-Wirtinger colorable.



A sequence of coloring moves can be notated as  $(A_0, f_0) \rightarrow (A_1, f_1) \rightarrow \cdots \rightarrow (A_m, f_m)$ , where  $f_i$  is a function from the subset of strands  $A_i$  to a finite set of  $k$  elements, which are the colors. To elaborate,  $(A_0, f_0)$  is the stage where only the seeds have been colored with the  $k$  colors. The strands that used to be attached to a pod will get repeated colors. The final stage  $(A_m, f_m)$  is when all the strands get colored.

In the proof of our main result, we embed each strand at a certain height dictated by the coloring moves. Thus, there is a function  $h: \{s_1, s_2, \dots, s_n\} \rightarrow \mathbb{R}$  from the set of strands that records the height of each strand  $s_i$ .

**Lemma 3.1.** *At any coloring stage, each color in the diagram is either (1) a connected arc if the seed corresponding to that color is an arc or (2)  $n$  disjoint arcs if the seed corresponding to that color is a pod of degree  $n$ .*

*Proof.* We verify this claim by induction on  $u$ , where  $u$  is the coloring stage. For the base case  $u = 0$ , this is the stage where no coloring move has been applied, so only the seeds are colored. The claim immediately holds by the way the seeds are defined. Now assume that the claim holds for  $u < t$  and consider the stage  $u = t > 0$ . By the definition of coloring move, there is a unique strand  $s_i$  adjacent to a strand in  $A_{t-1}$  such that  $A_t \setminus A_{t-1} = \{s_i\}$ . Thus,  $f_t^{-1}(c) = f_{t-1}^{-1}(c) \cup \{s_i\}$  for a particular color  $c$ . By the inductive hypothesis, we have that  $f_{t-1}^{-1}(c)$  is either  $n$  arcs if the seed corresponding to that color is a pod of degree  $n$ , or a connected arc if the seed corresponding to that color is an arc. Adding one arc  $s_i$  adjacent to some arcs in  $f_{t-1}^{-1}(c)$  preserves the property stated in the hypothesis.  $\square$

**Lemma 3.2.** *Suppose that a nontrivial spatial graph diagram  $D$  is  $k$ -colorable via the sequence  $(A_0, f_0) \rightarrow (A_1, f_1) \rightarrow \cdots \rightarrow (A_n, f_n)$ . At a crossing  $c$ , let  $s_p, s_q$ , and  $s_r$  denote an incoming understrand, an outgoing understrand, and an overstrand, respectively. If the understrands receive the same color  $j$  at stage  $n$ , then one of the following situations occurs:*

- (1) *the overstrand is not colored last,*
- (2) *the strands with the same color correspond to an unknotted component and  $c$  is the unique crossing with the property that  $h(s_r) \leq \min\{h(s_q), h(s_p)\}$ , or*
- (3) *the strands with the same color correspond to self-loops (that is, edges which connect a vertex to itself) in the graph connected to a pod and  $c$  is the unique crossing in a self-loop with the property that  $h(s_r) \leq \min\{h(s_q), h(s_p)\}$ .*

*Proof.* Suppose that  $h(s_r) \leq \min\{h(s_q), h(s_p)\}$ . First, suppose that  $s_p = s_q$ . Then, the lift of  $s_p = s_q$  is an unknotted component in 3-space. Furthermore, the only way to obtain a Wirtinger colorable diagram is to make  $s_p = s_q$  a seed strand. In this case, we get the conclusion (2). The uniqueness of the crossing with this property is automatic since this unknotted component only has one crossing with the rest of the diagram in which it is the understrand.

Now we may suppose that  $s_p \neq s_q$ . Without loss of generality, suppose that  $h(s_q) \leq h(s_p)$ . By Lemma 3.1, two cases can happen.

*Case 1 (the color  $j$  forms a connected arc because the corresponding seed is an arc):* The strand  $s_q$  receives its color from an adjacent strand  $s_{q_1}$  by a coloring move. There is also a stage in which  $s_{q_1}$  receives its color from an adjacent strand  $s_{q_2}$  by a coloring move. We can



continue in this fashion to see that there is a stage in which  $s_{q_k}$  receives its color from a seed. This seed may or may not be  $s_p$ . If it is  $s_p$ , then we have found an unknotted component. If not, then we can do the same backtracking process starting at  $s_p$  to reach the seed for the color  $j$ , forming an unknotted component. Note that the existence of another crossing with the property that  $h(s_r) \leq \min\{h(s_q), h(s_p)\}$  implies that there were at least two seed arcs. However, repeated colors are only allowed for pod seeds.

*Case 2 (the color  $j$  consists of multiple arcs converging to a pod):* This case is depicted in Figure 4. Essentially, we use a backtracking argument starting at  $s_q$  as in Case 1 until we reach a strand in the truncated diagram with an open end. Backtracking from  $s_p$  will also end at the same pod. This creates the desired loop in the graph. The existence of another crossing with the property that  $h(s_r) \leq \min\{h(s_q), h(s_p)\}$  is only possible if multiple pod seeds have the same color. However, our coloring rule dictates that there is only one arc or one pod such that all strands connected to it receive the color  $j$ .  $\square$

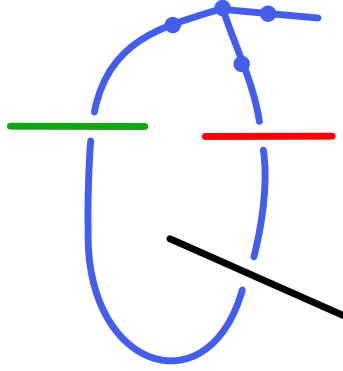


Figure 4: The crossing involving the black (uncolored) strand has the property that the overstrand  $s_r$  is not colored yet at this stage, but the understrands are colored with the same color. Here the vertex is put back into the truncated diagram for reference.

**Remark 3.3.** The uniqueness of a crossing for a color with the property that  $h(s_r) \leq \min\{h(s_q), h(s_p)\}$  will be used to ensure that there are the correct number of places to put a local minimum in the proof of Theorem 1.1.

**Proposition 3.4.** *For spatial graphs, the Wirtinger number is at most the bridge index.*

*Proof.* Given a spatial graph, suppose that its bridge index  $r$  is realized by a diagram  $D$ , and without loss of generality, let the number of upper pods and maxima be less than or equal to the number of lower pods and minima. Think of  $D$  as lying in the  $xy$ -plane. We can pull the upper pods and maxima to the same height  $y = a$ , and the lower pods and minima to the same height  $y = b$ . After making the  $r$  upper pods and maxima in the diagram seeds, the colorings can be extended to the entire diagram using only the coloring moves. To see this, observe that after removing the maxima, minima, and vertices of degree at least three at the pods, we obtain a braid diagram between  $y = a$  and  $y = b$ . Once the seeds are chosen,

all of the strands connected to the top endpoints of the braid diagram are colored. If the braid is slightly perturbed so that each crossing is at a distinct height, it is easy to see that the coloring can be extended at every crossing (see Figure 5 and its caption). We can also require that the lower pods are colored last. Therefore, the Wirtinger number of  $D$  is  $r$ .  $\square$



Figure 5: In a block of a braid diagram that contains only one crossing, there is only one strand that is not connected to the top dashed horizontal boundary. Such a strand is colored black to signify that it has not been colored yet. Thus, if the strands connected to the top are colored, then we just need one coloring move for each block of braid diagram.

**Theorem 1.1.** *For spatial graphs, the Wirtinger number equals the bridge index.*

*Proof.* By Proposition 3.4 we have that the Wirtinger number is at most the bridge index. For the other inequality, suppose we have a spatial graph with Wirtinger number  $n$  which is realized by a diagram  $D$ . We will construct an embedding of our graph in  $\mathbb{R}^3$  with bridge index  $n$ . Refer to Figure 6 throughout the proof for an example of how the embedding works.

We embed the strand that receives color at stage  $j$  in the plane  $z = -j$  in  $\mathbb{R}^3$ . Here, strands belonging to the same seed pod are on the same level. If the graph has  $m$  strands, we embed the diagram  $D$  itself in the level  $z = -m - 5$ . The exact level does not matter; the spatial graph will sit at or above level  $z = -m$  by construction, and we just wish to place the diagram below so that the graph projects down to the diagram. We denote the lift of the strand  $s_i$  in the diagram to the spatial graph by  $\tilde{s}_i$ .

At the moment, the embedded strands are all disconnected. Note that the disconnected places correspond to either a crossing in the diagram or the free ends coming from removing the vertices of the pods. To form an embedding of our spatial graph, we will connect up the strands crossing-by-crossing in such a way that our embedding has  $k$  upper pods and  $n - k$  local maxima, which will project down to seeds in the diagram. Then we will add in the vertices of the pods. For each crossing, this connection will happen in a cylinder  $B_\varepsilon^2(c) \times \mathbb{R}$ , where  $B_\varepsilon^2(c) \subset \{z = -m - 5\}$  is a open 2-disk neighborhood of the crossing  $c$  with radius  $\varepsilon$  chosen small enough so that it contains only the overstrand  $s_k$  and the two adjacent understrands  $s_i$  and  $s_j$ . Each crossing falls into one of the following two cases.

*Case 1:* Assume that at the end of the coloring process, the color of  $s_i$  is not the same as the color of  $s_j$ . In this case, we connect one end of the lift of  $s_i$  to an end of the lift of  $s_j$  with an arc  $s_{ij}$  so that exactly one local minimum is created. We cannot use a monotonic arc as the height of the overstrand is too low. More precisely,  $s_{ij}$  is constructed as a union of two arcs. One of the arcs starts from  $\tilde{s}_i$ , and goes monotonically down to a point  $x_{ij}$ , where  $x_{ij}$  projects down to  $c$  in the diagram. The other arc goes from  $x_{ij}$  monotonically up to  $\tilde{s}_j$ . We

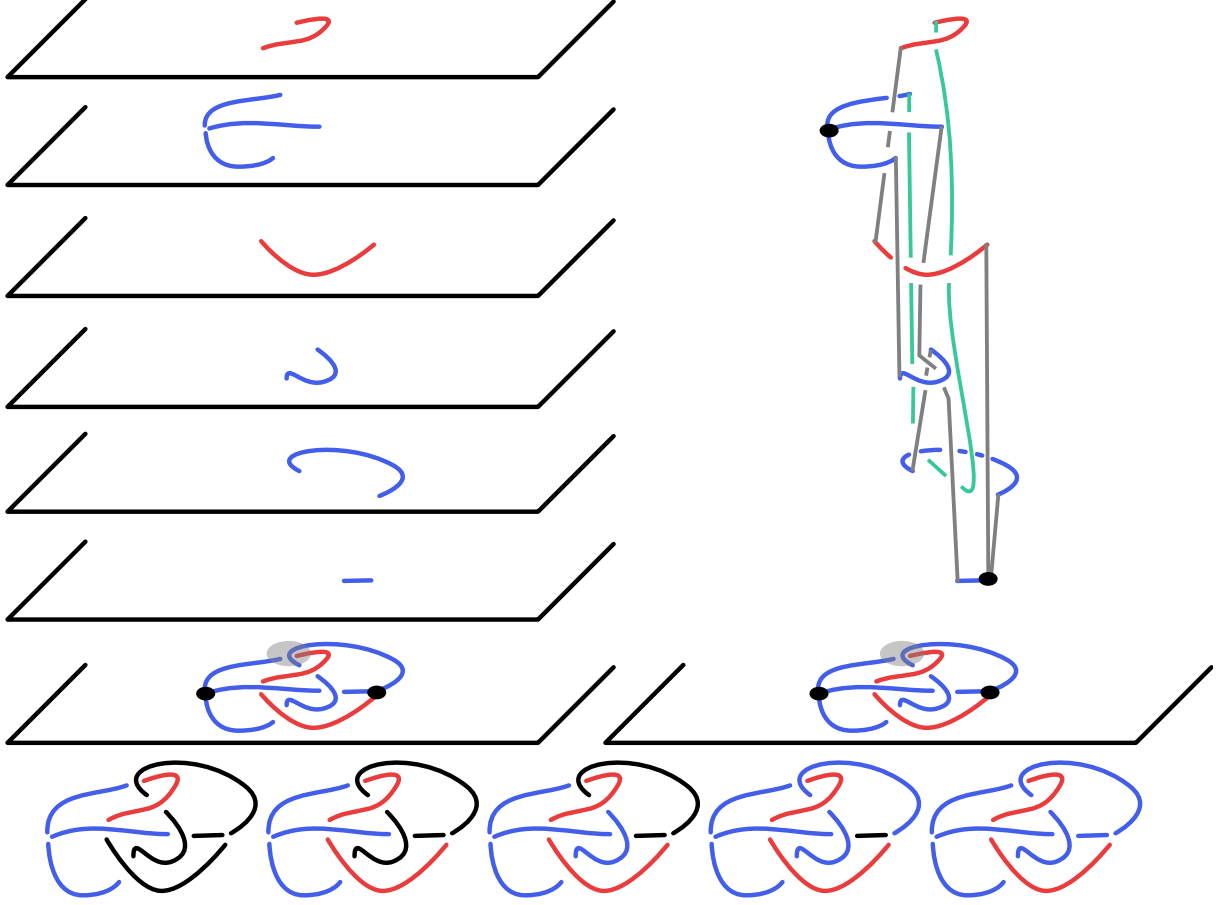


Figure 6: A schematic showing that the unique multi-colored crossing (highlighted in gray) corresponds to connecting up the disjoint strands with a new strand (colored green) with a single local minimum.

note that there are many choices for where to put  $x_{ij}$ . For instance, putting  $x_{ij}$  at the height  $z = -m - 4$  will work. In Figure 6, the point  $x_{ij}$  is the local minimum of the green arc.

*Case 2:* Assume that at the end of the coloring process, the color of  $s_i$  is the same as the color of  $s_j$ . In this case, by Lemma 3.2, there are two subcases.

*Subcase 2.1:* Suppose it holds that  $h(s_k) > \min\{h(s_i), h(s_j)\}$ . Without loss of generality, suppose that  $\tilde{s}_i$  is lower than  $\tilde{s}_j$ . For this case, the connection arc can be created without introducing a local maximum or a local minimum because the overstrand is not colored last. Formally, we construct  $s_{ij}$  as a monotonically decreasing arc from an endpoint of  $\tilde{s}_j$  to an endpoint of  $\tilde{s}_i$  contained in  $B_\epsilon^2(c) \times \mathbb{R}$  so that a point on  $s_{ij}$  orthogonally projects to the crossing  $c$ . For a concrete demonstration, please consult Figure 6, where every crossing except the one highlighted with the gray oval falls into this subcase.

*Subcase 2.2:* Assume that at the end of the coloring process, the color of  $s_i$  is the same as the color of  $s_j$  and  $h(s_k) \leq \min\{h(s_i), h(s_j)\}$ . Then by Lemma 3.2, we either get an unknotted component or a self-loop (that is, an edge which connects a vertex to itself) in our spatial graph.

In the former case, Lemma 3.2 implies that there is exactly only one crossing  $c$  with this

property such that the overstrand receives the color last. We then connect the strand  $\widetilde{s}_i$  to  $\widetilde{s}_j$  by two arcs as in Case 1 so that this crossing  $c$  corresponds to exactly one local minimum in the lift. In the latter case, [Lemma 3.2](#) implies that there is exactly one crossing  $c_i$  for each self-loop  $i$ . We also connect the strand  $\widetilde{s}_i$  to  $\widetilde{s}_j$  by two arcs as in Case 1 so that each crossing  $c_i$  corresponds to exactly one local minimum in the lift.

After all open ends are joined up at each crossing, we can add vertices to the levels containing multiple strands. After a slight perturbation, these vertices correspond to upper pods. The lifts of the other seed strands, where each seed was one connected arc in the initial coloring stage, can be perturbed slightly to be local maxima. The multi-color crossings lift to local minima.

The remaining disconnected places in the lift project down to vertices of non-seed pods in the diagram. For such a vertex  $v$ , let the lifts of the strands be  $\{\widetilde{s}_{i_1}, \widetilde{s}_{i_2}, \dots, \widetilde{s}_{i_d}\}$ , where  $d$  is the degree of the corresponding non-seed pod. To create our desired embedding, we place a point  $\tilde{v}$  at the free end of the lowest arc, say  $s_{i_d}$  without loss of generality. Then, add an arc from the free end of  $\{\widetilde{s}_{i_1}, \widetilde{s}_{i_2}, \dots, \widetilde{s}_{i_{d-2}}, \widetilde{s}_{i_{d-1}}\}$  monotonically down to  $\tilde{v}$ . Each such  $\tilde{v}$  will correspond to lower pods after a slight perturbation. This completes our embedding: after possibly some additional slight perturbations, we have put our spatial graph in bridge position with bridge index  $n$ .  $\square$

## 4 Lower bounds

The following techniques are computable quantities that bound the bridge index of graphs from below. In the setting of links, we know by experimentation that depending on the link types, one method may be more effective than the others [\[NPV24\]](#). That is, in some instances the computer code finds enough quandle colorings, but not a rank bound, and vice versa.

### 4.1 Quandle colorings

In [\[FM07; Nie10\]](#) the authors generalized knot quandles to spatial graphs.

**Definition 4.1.** A *quandle* is a set  $X$  equipped with a binary operation  $\triangleright$  satisfying the following axioms.

- (1)  $x \triangleright x = x$  for all  $x \in X$ .
- (2) The map  $f_y : X \rightarrow X$  defined by  $f_y(x) = x \triangleright y$  is invertible for all  $y \in X$ .
- (3)  $(x \triangleright y) \triangleright z = (x \triangleright z) \triangleright (y \triangleright z)$  for all  $x, y, z \in X$ .

A *consistent labeling*<sup>1</sup> of a diagram by a quandle is an assignment of a quandle element to each strand, such that strands connected to the same vertex receive the same label, and the relation in [Figure 7](#) is satisfied at each crossing. It can be shown that for knots and links, the number of consistent labelings is unchanged by the Reidemeister moves. For general spatial graphs, however, this is no longer true.

The move for spatial graphs which interacts with the vertices, as seen in [Figure 8](#), forces the quandles that are suitable for spatial graphs to have a more restrictive form. For instance,

---

<sup>1</sup>Various authors also use the term *quandle coloring*, *X-coloring*, or simply *coloring* for this

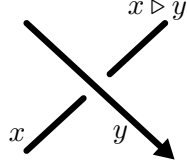


Figure 7: The relation at each crossing in a quandle labeling.

the coloring by the dihedral quandle  $R_3$  (Fox 3-coloring) no longer works for some graphs, such as those containing the situation in Figure 8, due to this new graph move.

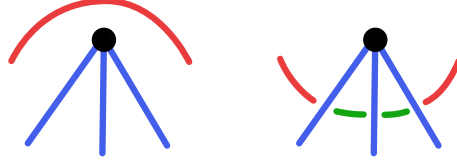


Figure 8: For a quandle coloring to work, the strands near a crossing need to all receive the same color or all distinct colors. On the left, the strands are disjoint and the strands adjacent to a pod receive one color. If the other strand receives a different color, after we perform a move that does not change the graph type, we are forced to have a crossing that uses only two colors.

On the other hand, the order four Alexander quandle with the following multiplication table works for the new graph move on a degree three vertex.

$$\begin{aligned}
 0 &= 0 \triangleright 0 = 1 \triangleright 2 = 2 \triangleright 3 = 3 \triangleright 1 \\
 1 &= 0 \triangleright 3 = 1 \triangleright 1 = 2 \triangleright 0 = 3 \triangleright 2 \\
 2 &= 0 \triangleright 1 = 1 \triangleright 3 = 2 \triangleright 2 = 3 \triangleright 0 \\
 3 &= 0 \triangleright 2 = 1 \triangleright 0 = 2 \triangleright 1 = 3 \triangleright 3
 \end{aligned}$$

This motivates the following definition.

**Definition 4.2.** An  $n$ -quandle is a set  $X$  equipped with a binary operation  $\triangleright$  satisfying the quandle axioms in Definition 4.1 and one additional axiom  $((x \triangleright y) \triangleright y) \triangleright \cdots \triangleright y = x$  for all  $x, y \in X$ , where the total number of quandle operations in the additional axiom is  $n$ .

We remark that in [Nie10], the authors allow edges coming out of the same vertex to have different labels, but for our lower bound of the bridge index  $\beta$ , we will just consider the case where the elements at the edges around the same vertex are the same.

**Proposition 4.3.** Let  $X$  be a finite  $n$ -quandle of order  $|X|$ . Let  $Col_X(G)$  denote the coloring number of the spatial graph  $G$  by  $X$ . Then  $Col_X(G) \leq |X|^{\beta(G)}$ . In other words,

$$\log_{|X|} Col_X(G) \leq \beta(G).$$

*Proof.* Some elements of this proof appeared in Proposition 3.4, but instead of just using colors, we are coloring with quandle elements. There are  $|X|$  possibilities to assign an element of  $X$  to an upper pod or a local maximum. In a bridge index minimizing diagram, there are  $|X|^{\beta(G)}$  ways to assign elements of  $X$  to the upper pods and local maxima. This assignment determines all of the other labels in the diagram as argued in Proposition 3.4.  $\square$

We now provide a lower bound for the bridge index of vertex sums of spatial graphs (recall [Section 2.1](#)) in terms of quandles, which will be useful to us in [Section 5](#). The argument is based on [\[CSV16\]](#). The key is the existence of quandles called *homogeneous quandles*, which have the property that for any quandle elements  $x, y$ , there is an automorphism  $h$  such that  $h(x) = y$ . Note that the map  $f_y$  sending  $x$  to  $x \triangleright y$  in the second axiom of [Definition 4.1](#) is an example of an automorphism by the way the axiom is stated. The reader can check from the table before [Definition 4.2](#) that the Alexander quandle of order four is homogeneous.

**Proposition 4.4.** *Let  $X$  be a homogeneous  $n$ -quandle, and  $G \#_n G'$  be the  $n$ -valent vertex sum of spatial graphs  $G$  and  $G'$ . Then*

$$\text{Col}_X(G \#_n G') = \frac{1}{|X|} \text{Col}_X(G) \cdot \text{Col}_X(G').$$

Thus, we achieve the lower bound

$$\log_{|X|} \text{Col}_X(G) + \log_{|X|} \text{Col}_X(G') - 1 \leq \beta(G \#_n G').$$

*Proof.* The number of colorings where a fixed color  $x$  is assigned to the strands adjacent to a vertex  $v$  is precisely  $\text{Col}_X(G)/|X|$ . To see this, observe that the number of colorings  $\text{Col}_X(G) = \sum_y \text{Col}_X(G, y)$ , where  $\text{Col}_X(G, y)$  denotes the number of colorings such that the strands near  $v$  get the label  $y$ . We can get another coloring in which the strands adjacent to  $v$  are colored  $z \neq y$  by applying an automorphism  $h$  such that  $h(y) = z$ , which exists by the homogeneity assumption. Thus,  $\text{Col}_X(G) = |X| \text{Col}_X(G, y)$ .

Now we consider the vertices of  $G$  and  $G'$  that we will do the vertex sum along. For any fixed coloring of  $G$ , we look at the coloring at the vertex; call it  $x$ . Then there are  $\frac{1}{|X|} \text{Col}_X(G')$  colorings for  $G'$  that have the coloring  $x$  at the vertex to match up with  $G$ . Therefore,  $\text{Col}_X(G \#_n G') = \frac{1}{|X|} \text{Col}_X(G) \cdot \text{Col}_X(G')$ . The stated inequality comes from combining this equation with the result of [Proposition 4.3](#) and simplifying.  $\square$

## 4.2 Meridional rank

The fundamental group of the complement of a spatial graph  $G$  in  $S^3$  can be computed via the Wirtinger algorithm in a similar way to the computations for knots and links. Each arc of a spatial graph diagram gives a generator, and each crossing gives a relation of the form  $x_i x_j x_i^{-1} x_k^{-1}$ . At a vertex, we have a new type of relation of the form  $x_{i_1}^{\epsilon_1} x_{i_2}^{\epsilon_2} \cdots x_{i_n}^{\epsilon_n}$ , where the generators are listed in order as we go clockwise around a vertex, and  $\epsilon_i$  is 1 (resp.  $-1$ ) if the arc is directed into the vertex (resp. directed out of the vertex). See [Figure 9](#).

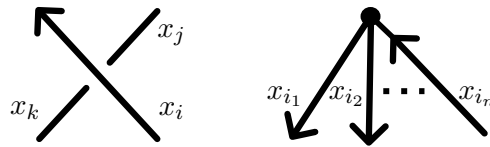


Figure 9: On the left is the relation  $x_i x_j x_i^{-1} x_k^{-1}$  at each crossing. On the right is the relation  $x_{i_1}^{\epsilon_1} x_{i_2}^{\epsilon_2} \cdots x_{i_n}^{\epsilon_n}$  at a vertex.

The technique of bounding the number of handles of knotted objects by the meridional rank of the fundamental group has been used before in other settings such as classical links [BBK21] and surface-links [JP24]. We now adapt the method to the setting of spatial graphs.

In [Liv95] Livingston defined the *vertex constant group*  $\pi^*$  to be the quotient of  $\pi_1(S^3 \setminus G)$  defined by setting all meridians at each vertex equal to each other. We are interested in bounding the rank of the vertex constant group, where our generating set consists of meridians. We achieve this by searching for a consistent labeling of our diagram by reflections in a Coxeter group  $C(\Delta)$ . This will produce a surjective homomorphism from  $\pi^*$  to  $C(\Delta)$ .

**Definition 4.5.** Recall that a presentation of a *Coxeter group*  $C(\Delta)$  can be obtained from a weighted graph  $\Delta$  as follows. Label the vertices of  $\Delta$  as  $x_1, x_2, \dots, x_n$ , which will be the generators. If there is an edge with weight  $w$  connecting  $x_i$  to  $x_j$ , then we have a relation  $(x_i x_j)^w$  in the presentation. Additionally, the relations also include  $x_i^2$ , for  $i = 1, 2, \dots, n$ .

The number of vertices of  $\Delta$  is referred to as the *reflection rank*. The following lemma is important in obtaining our bound.

**Lemma 4.6** ([FT10, Lem. 2.1]). *If all edge weights of  $\Delta$  are at least two, then the reflection rank equals the minimal number of reflections needed to generate  $C(\Delta)$ .*

**Definition 4.7.** A labeling of arcs in a spatial graph diagram  $D$  is *consistent* if at each crossing where the overstrand is labeled with an element  $g$  and the two understrands are labeled  $h$  and  $k$ , we have that  $ghg = k$ . We say that the label *generates* the group if every element of  $C(\Delta)$  can be written as a product of the elements that appear as labels along with their inverses.

Note that in Coxeter groups the generators are involutions, so the role of  $h$  and  $k$  can be interchanged in the definition above.

**Proposition 4.8.** *If a diagram  $D$  representing a spatial graph  $G$  can be labeled by  $n$  reflections from a Coxeter group  $C(\Delta)$  with reflection rank  $n$ , then  $\beta(G) \geq n$ .*

*Proof.* In the same spirit as Proposition 3.4 and Proposition 4.4, the labels on the upper pods and maxima determine all the other labels. The difference is that we use a labeling by Coxeter groups in this setting. Thus, these labels generate  $C(\Delta)$ . We then appeal to Lemma 4.6 to conclude that we need at least  $n$  reflections to generate  $C(\Delta)$ .  $\square$

## 5 Computations

In this section, we use our techniques to estimate or provide exact values for the bridge indices of many different examples of knotted spatial graphs. In particular, although the following statement also follows from other techniques, our coloring and meridional rank techniques give short arguments, as we will see in Corollary 5.9, Corollary 5.13, and Corollary 5.18.

**Corollary 1.2.** *The bridge index of a spatial graph can be arbitrarily large.*

Refer to Section 2.1 for a review of the spatial graph terminology we use throughout this section. We break into various subsections according to the type of construction, but start first with a relatively simple example.



**Example 5.1** (Almost unknotted graphs from unlinks). As a warmup, Figure 10 gives an almost unknotted handcuff graph (left) and an almost unknotted  $\Theta$ -graph (right). Both of these well-known examples – for instance the  $\Theta$ -graph is the Kinoshita graph [Kin58; Kin72] – were constructed by adding an edge to an unlink, and both have bridge index 2. These diagrams are already in bridge position demonstrating this index, but this can also be verified by finding 2-Wirtinger colorings of the diagrams. The lower bound comes from the fact that there is a nontrivial coloring by the Alexander quandle of order four from Section 4.1. Note that the number of crossings in each column of twists can be systematically increased and we still retain the consistency of the coloring. By systematic, we mean that if there are three crossings originally, we can keep adding a multiple of three crossings.

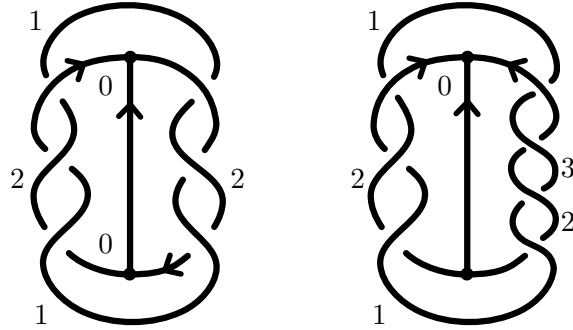


Figure 10: A quandle colored almost unknotted handcuff graph (left) and a quandle colored almost unknotted  $\Theta$ -graph (right), both with bridge index 2.

## 5.1 Python code

We implemented our algorithm in Python to compute upper bounds for the Wirtinger numbers of arbitrary  $\Theta_n$ -graphs ( $n \leq 26$ ). Our algorithm generalizes coloring algorithms used to compute bounds for the Wirtinger numbers for knots and links. We refer readers to [Bla+20b; LPV24] for details on the knot and link cases. Our Python code can be found at <https://github.com/hanhv/graph-wirt>. While the full detail can be found in the URL, we also give a summary here.

### Notation setup

Due to the lack of spatial graph tabulations, we generate Gauss codes of some spatial graphs from those of links.

**Definition 5.2.** A *Gauss code* for an  $m$ -component link is a list of  $m$  lists of positive and negative integers such that for all  $k \neq 0$ ,  $|k| \leq m$ , both  $k$  and  $-k$  appear once each among the lists.

**Definition 5.3.** A *Gauss code* for a spatial graph is a list of  $n$  lists, where each list corresponds to an edge of the graph. Each edge joins two vertices and includes information about the crossings it passes through.

For  $n \leq 26$ , a Gauss code for a  $\Theta_n$ -graph contains  $n$  lists, each corresponding to an edge in the graph. Each edge of the graph is represented by a list of numbers and symbols in the following way.

- The list starts and ends with a symbol in the form of a letter-number pair, such as **a1** or **b2**. The letter designates the direction, represented by alphabet letters, and the number following the letter indicates a vertex of the graph. The vertex number is positive.
- The numbers  $|k| \leq m$ , where  $k$  is non-zero and different from the vertex number, correspond to crossings. For a valid Gauss code, every integer from  $k \leq |m|$ , excluding zero and the vertex numbers, must appear exactly once across the entire code.

For example, the following Gauss code

```
gauss_code = [
    [a1, 3, -4, a2],
    [b1, -5, 6, 7, -8, 9, -7, 10, -11, 12, -10, -13, 14, b2],
    [c1, -9, 8, -3, 5, -6, 13, -14, 4, -12, 11, c2]
]
```

corresponds to the graph shown in [Figure 11](#).

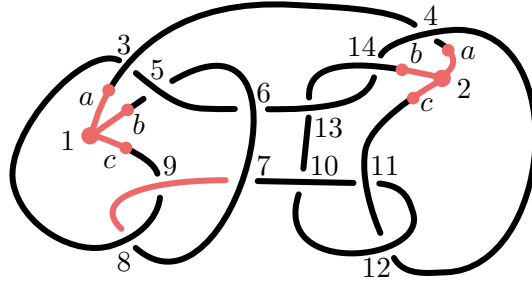


Figure 11: Example of a Gauss code. This diagram is 3-Wirtinger colorable using the seed  $\{[a1, b1, c1], [a2, b2, c2], \{-8, 9, -7\}\}$ , which is colored pink.

## Generating Gauss codes of $\Theta_4$ -graphs from two-component links

First we extract two-component link diagrams from the link table provided by SnapPy [\[Cul+24\]](#). Each of these links takes the form of a Gauss code made up of two lists of numbers. Selecting a two-component link, by “singularizing” we turn two crossings between components into 4-valent vertices. Here, a pair of crossings  $(x, y)$  is considered *singularizable* if both  $x$  and  $y$  appear in one component, while  $-x$  and  $-y$  appear in the other component. We only choose singularizable pairs that are of distance at least four apart (this is optional), ensuring that each edge of the graph contains at least four crossings. By singularizing a pair of crossings  $i$  and  $j$ , we split each component of the link, viewed as a cyclic list, into two parts with endpoints at  $i$  and  $j$ . This has the effect of turning the two-component link into a  $\Theta_4$ -graph.

## Computing the Wirtinger number of a graph diagram

The program begins by identifying all strands in the Gauss code, which can be classified as pods (arcs in the neighborhood of a vertex), arcs connecting the endpoints of pods to undercrossings, or arcs connecting two undercrossings. It first sets  $k = 1$  and generates a list of *seeds*, which are combinations of  $k$  strands, ensuring that at least one pod is included in each combination. (Our algorithm does not require this, but adding in this requirement will still produce a viable upper bound.) For each seed, it colors the arcs in the seed and creates a truncated version of the graph by removing any pods that are not part of the selected seed. The program then attempts to maximally extend this truncated graph through two types of coloring moves: one that extends from the endpoint of a pod and another that extends from an undercrossing if its corresponding overstrand is colored. If the entire truncated graph can be colored, the function returns  $k$ . If not, it tries the next seed. Should no combination successfully color the truncated graph, the algorithm increments  $k$  and repeats the process.

## Output

We extracted and computed the Wirtinger numbers for over 260,000  $\Theta_4$ -graph diagrams.

## 5.2 Hara's graphs and modifications

**Example 5.4** (Hara's graphs). The family of almost unknotted  $\Theta_4$ -graphs given by Hara [Har91, Fig. 2] all have bridge index 2, which can be quickly verified by finding 2-Wirtinger colorings of the diagrams. This is perhaps surprising, as these particular diagrams have many more local maxima and minima.

**Example 5.5** (Modifications of Hara's graphs). We create two families of spatial graphs by modifying Hara's  $\Theta_4$ -graphs from the previous example; however these families are *not* almost unknotted. For both families we give upper bounds for their bridge indices, which can be verified by finding corresponding Wirtinger colorings. In both cases, we conjecture that this upper bound is in fact the bridge index.

For the sake of simplicity, we depict both families as coming from  $\Theta$ -graphs rather than  $\Theta_4$ -graphs, but both could be further extended by adding more edges in analogous ways. This would likely not change the bridge index. Note that with this change, we can (perhaps more appropriately) think of these families as modifications of a Kinoshita-Wolcott graph [Kin58; Kin72; Wol87] (see [Jan+16, Fig. 1]).

First we alter Hara's graphs by replacing the braids on two strands with braids on  $n$  strands as in Figure 12 (left). In the specific instance shown in Figure 12 (left) the constituent knots are all  $5_2$ .

**Fact 5.6.** *Let  $G_n$  be the  $\Theta$ -graph obtained from Hara's graphs by replacing the braids on two strands with braids on  $n$  strands. Then the bridge index of  $G_n$  is less than or equal to  $n$ .*

Second we alter Hara's graphs by taking  $n$  parallel copies of each edge as in Figure 12 (right). For the instance shown in Figure 12 (right) every pair of edges forms an unknot, but not every proper subgraph is trivial: when one edge is deleted, the remaining parallel edge still causes a problem.

**Fact 5.7.** *Let  $G_n$  be the  $\Theta_{3n}$ -graph obtained from Hara's graphs by taking  $n$  parallel copies of each edge. Then the bridge index of  $G_n$  is less than or equal to  $n + 1$ .*

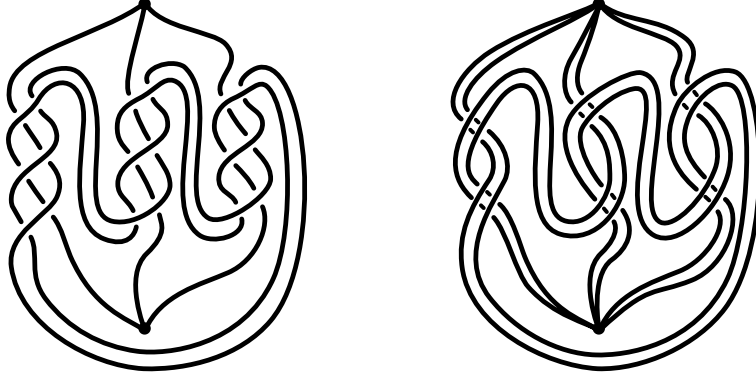


Figure 12: Some spatial graphs constructed by modifying Hara's graphs. On the left we modify by changing the number of strands in the twist regions, and on the right we modify by adding parallel edges.

### 5.3 Families from vertex sums

**Example 5.8** (Vertex sums of Suzuki's graph). Take  $n$  copies of the almost unknotted Suzuki  $\Theta_4$ -graph [Suz84], as shown in Figure 13. Consider the quandle  $(\{0, 1, 2\}, \triangleright)$ , where  $x \triangleright y = 2y - x \pmod{3}$ . It can be shown that this quandle is homogeneous (see [FT24], for example). In Figure 13 we give three consistent colorings of the graph by this quandle; then by permuting the colors, we have a total of nine possible colorings.

Taking the vertex sum of  $n$  copies of the graph, we obtain a diagram with bridge index  $n + 1$ . Using Proposition 4.4, we get that the number of colorings of the resulting vertex sum is  $3^{n+1}$ . Then by Proposition 4.3, the bridge index is precisely  $n + 1$ . Thus we have shown the following.

**Corollary 5.9.** *Let  $G_n$  be the  $\Theta_4$ -graph obtained by taking the vertex sum of  $n$  copies of Suzuki's graph. Then the bridge index of  $G_n$  is  $n + 1$ .*

**Example 5.10** (Vertex sums via clasp moves). The clasp move [SW90] (see [Jan+16, Fig. 3]), is a well-known move which preserves almost unknottedness of  $\Theta$ -graphs. We will use this to build a family of graphs as follows. First construct an almost unknotted  $\Theta$ -graph by performing the clasp move on a slightly isotoped trivial  $\Theta$ -graph as in Figure 14 (left). Then let  $G_n$  be the almost unknotted  $\Theta$ -graph obtained by repeating this procedure several times on the same graph, such that the clasps are “stacked” on top of each other, as indicated in Figure 14 (right). Note that the resulting graph can also be obtained by taking the vertex sum of  $n$  copies of the original graph. In this sense, we can view these vertex sums as coming from clasp moves.

**Fact 5.11.** *Let  $G_n$  be the almost unknotted  $\Theta$ -graph obtained by taking the vertex sum of  $n$  copies of the graph obtained from the clasp move in Figure 14 (left) on top of each other, as in Figure 14 (right). Then the bridge index of  $G_n$  is less than or equal to  $2n + 1$ .*

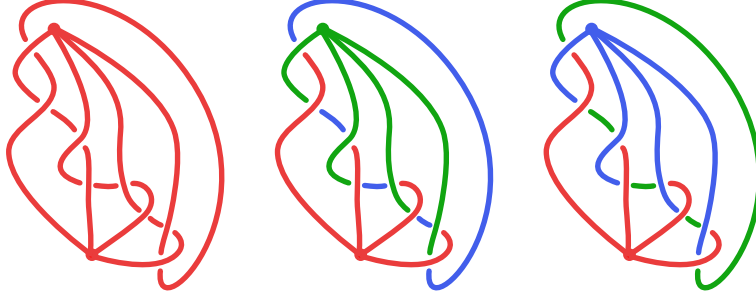


Figure 13: For a Suzuki  $\Theta_4$ -graph, we see that the number of colorings where the strands next to a particular vertex are labeled by a fixed element of the dihedral quandle of order three is three. (Here we use colors to represent the labelings by the quandle.) Thus by permuting the colors, we have a total of nine colorings.

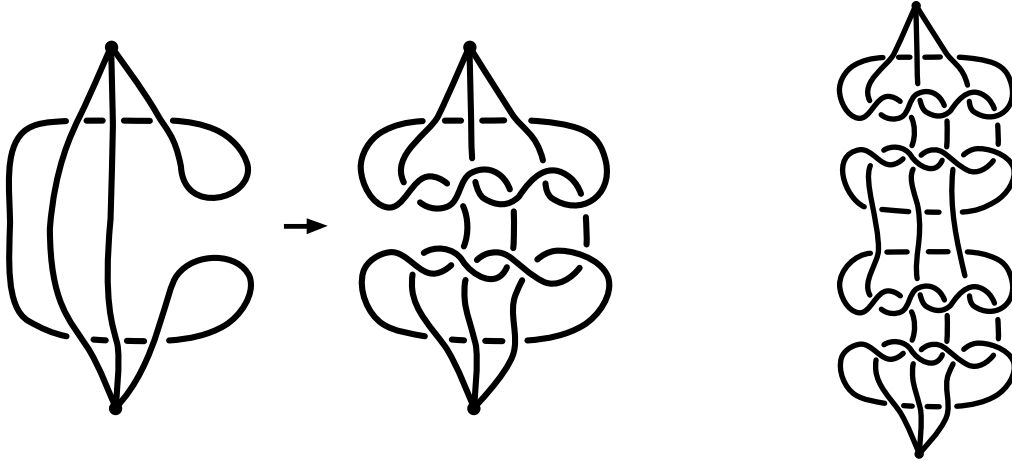


Figure 14: Performing the clasp move to construct a new almost unknotted  $\Theta$ -graph (left). A  $\Theta$ -graph constructed by taking the vertex sum of copies of the graph obtained from the clasp move, or equivalently, performing the clasp move multiple times (right).

This family  $G_n$  fits into a more general family of almost unknotted  $\Theta_m$ -graphs, constructed analogously, but we expect the bridge index to remain  $2n + 1$  regardless of  $m$ .

**Example 5.12** (More vertex sums via clasp moves). We can construct a somewhat simpler family of almost unknotted  $\Theta$ -graphs by performing “half” of the clasp move in the initial graph, as in Figure 15 (left). Note that this graph fits into the family of Kinoshita-Wolcott graphs [Kin58; Kin72; Wol87] (see [Jan+16, Fig. 1]), and could be seen as being obtained from this perspective. Let  $G_n$  be the family obtained from taking  $n$  vertex sums of this graph, as indicated in Figure 15 (right).

In Figure 16 we give four consistent labelings of  $G_1$  by the Alexander quandle of order four from Section 4.1. It is well-known that this quandle is homogeneous, but the readers can also verify from the table before Definition 4.2 that for any  $x$  and  $z$ , there is a  $y$  such that  $x \triangleright y = z$ . Observe that by permuting labels, the total number of colorings of  $G_1$  is 16. By Proposition 4.4, the number of colorings of  $G_n$  is  $4^{n+1}$ , and by a combination of the lower

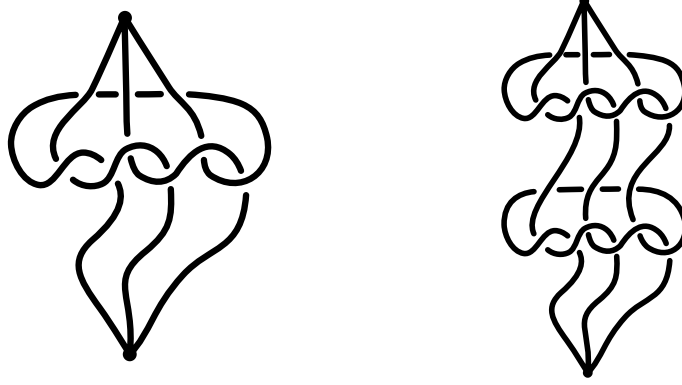


Figure 15: The result of performing “half” of the clasp move to construct a new almost unknotted  $\Theta$ -graph (left). A  $\Theta$ -graph constructed by taking the vertex sum of  $n$  copies of the graph on the left, or equivalently, performing the “half” clasp move multiple times (right).

bound coming from [Proposition 4.3](#) and the upper bound coming from our algorithm, we see that the bridge index is precisely  $n + 1$ .

**Corollary 5.13.** *Let  $G_n$  be the almost unknotted  $\Theta$ -graph obtained by taking the vertex sum of  $n$  copies of the graph obtained from the clasp move in [Figure 15](#) (left) on top of each other, as in [Figure 15](#) (right). Then the bridge index of  $G_n$  equals  $n + 1$ .*

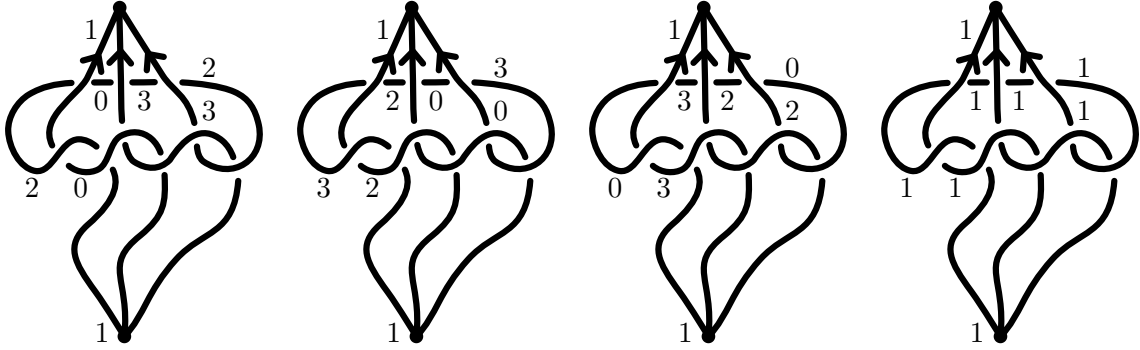


Figure 16: Four consistent labelings of the graph in [Figure 15](#) (left) by the Alexander quandle of order four. Thus by permuting the labels, we have a total of nine colorings.

## 5.4 Eulerian spatial graphs from links

**Example 5.14** (More clasping). We construct two spatial graphs by performing “clasp-like” moves in a different sense than [Example 5.10](#).

First, consider the two-component spatial graph shown in [Figure 17](#) (left). Note that this graph is almost unknotted and, perhaps surprisingly, has bridge index 3 (which we will verify in [Example 5.17](#)). Further note that changing the number of twists in various places, as long

as each twist region remains an odd number of half-twists, will not change the linkedness, almost unknottedness, or bridge index of the graph.

Second, consider the  $\Theta_4$ -graph shown in Figure 17 (right). Note that this graph is *not* almost unknotted, but it also has bridge index 3. Further note that changing the number of twists in various places, as long as the parity of the number of half-twists of each twist region is preserved, will not change the bridge index of the graph.

For both graphs, if we create a family of graphs from them by adding further pairs of edges that are clasped together in the same way as the two pairs in the given graphs, the upper bound for the bridge index coming from our algorithm increases accordingly, and we conjecture that this upper bound is in fact the bridge index. Note however that the almost unknottedness of the spatial graph in Figure 17 (left) will be destroyed once more edges are added.

**Fact 5.15.** *Let  $G_n$  be the  $\Theta_{2n}$ -graph obtained by increasing the number of edges of either of the graphs in Figure 17 as described above. Then the bridge index of  $G_n$  is less than or equal to  $n + 1$ .*

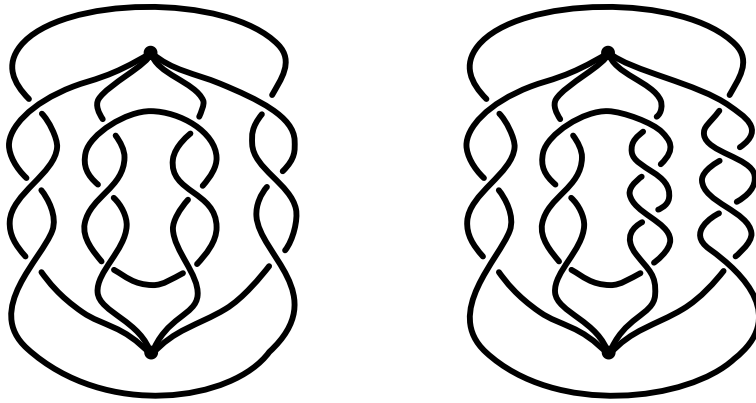


Figure 17: Two more spatial graphs constructed from “clasp-like” moves.

Another way of viewing the construction in Example 5.14 is by fusing pairs of maxima and minima of pretzel links, which leads us to a more general construction. Recall that a graph is *Eulerian* if every vertex has even degree. There are numerous collections of knots and links that have an arbitrarily large number of quandle colorings or admit Coxeter quotients with arbitrarily large reflection rank. Therefore, the knots in these collections have arbitrarily large bridge index. Taking a knot and fusing pairs of local maxima or pairs of local minima together creates an Eulerian graph with degree four vertices (see Figure 18). In various cases, we can obtain an almost unknotted graph this way. Furthermore, we inherit some lower bounds from the links.

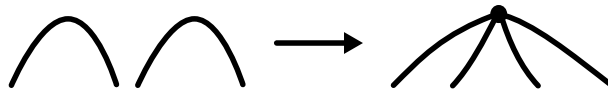


Figure 18: Fusing two maxima to form a vertex of degree four.



Recall from [Section 4.2](#) that we can use labelings by a Coxeter group to obtain lower bounds for bridge indices. Following [\[BKM24\]](#), we call a surjective group homomorphism  $\rho: \pi_1(S^3 \setminus L) \twoheadrightarrow C$  from the fundamental group of a link to a Coxeter group  $C$  a *good quotient* if meridians are mapped to reflections.

**Proposition 5.16.** *Suppose that  $\rho$  is a good quotient for a link  $L$ . Let  $D$  be a bridge index minimizing diagram of  $L$ . Let  $G_L$  be a spatial graph represented by the result of fusing the two local extrema of  $D$  with two different labels together (see [Figure 19](#) for a demonstration). Then  $\rho$  induces a surjective homomorphism  $\pi_1(S^3 \setminus G_L) \twoheadrightarrow C$  sending meridians around the fusing vertex to a reflection.*

*Proof.* Take two local extrema in  $D$  associated to reflections  $x, y$ . After fusing, we can label the strands connected to the newly created degree four vertex as  $y$ . The presentation of the Coxeter group that  $\rho$  surjects to is changed from  $\langle x_1, x_2, \dots, x_{n-2}, x, y \mid R, (xx_i)^{w_i}, (yx_j)^{w_j} \rangle$  to  $\langle x_1, x_2, \dots, x_{n-2}, y \mid R, (yx_i)^{w_i}, (yx_j)^{w_j} \rangle$ . Fusing the two extrema of  $D$  changes the graph  $\Delta$  by a collapsing move as shown in [Figure 20](#). In particular, we set two generators equal to each other. Thus  $\rho$  induces a surjective homomorphism from the fused spatial graph to a Coxeter group with one fewer reflection rank.  $\square$

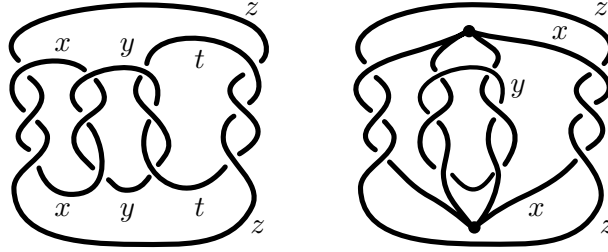


Figure 19: Fusing two maxima of a generalized pretzel link together. Before fusing, we have a good quotient to a Coxeter group of reflection rank 4. After fusing, we have a good quotient to a Coxeter group of reflection rank 3.

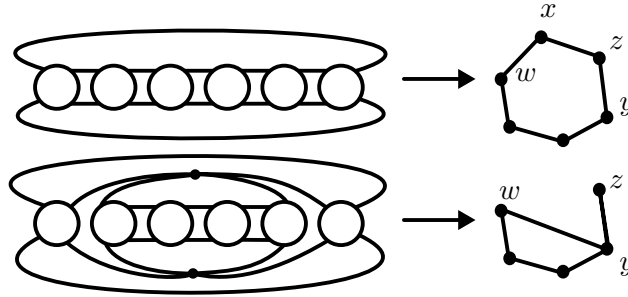


Figure 20: Fusing two maxima affects  $\Delta$  (from [Definition 4.5](#)) by identifying two vertices and preserving adjacency. For instance, the reflection  $x$  was connected to  $w$  and  $z$  beforehand. After fusing, we have that  $y$  is connected to  $w$  and  $z$ . The circles in the diagrams on the left hand side represent different rational tangles.

**Example 5.17** (Graphs from Montesinos links). Consider the left picture of [Figure 21](#). Once rational tangles are added in the circles, this is a Montesinos link, and the authors of [\[BBK21\]](#) have shown that it admits a good quotient. In particular, the meridional rank and the bridge index is  $n$ , where  $n$  is the number of rational tangles inserted. Each maximum is associated to a reflection. Using [Proposition 5.16](#), we can obtain a spatial graph with bridge index  $n - 1$ . Thus we can construct infinitely many graphs for which our technique can produce the exact bridge index, where in this case, the graphs are not just coming from a family of vertex sums as in previous examples. Of course, some choices will not give an almost unknotted graph, but some choices, such as [Figure 17](#) (left), will.

**Corollary 5.18.** *Let  $G_n$  be the spatial graph obtained from fusing the maxima and minima of a Montesinos link with  $n$  rational tangles. Then the bridge index of  $G_n$  is  $n - 1$ .*

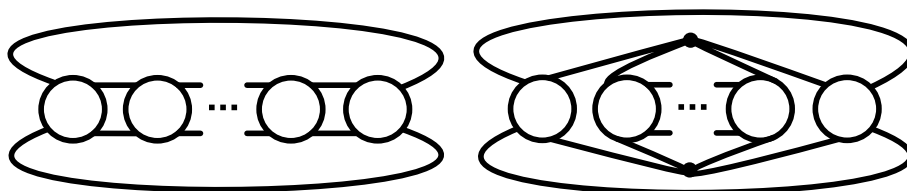


Figure 21: A schematic to construct infinitely many graphs for which our technique can produce the exact bridge index. The circles represent different rational tangles.

## References

- [Ada+12] Colin Adams, Michelle Chu, Thomas Crawford, Stephanie Jensen, Kyler Siegel, and Liyang Zhang. “Stick index of knots and links in the cubic lattice.” In: *Journal of Knot Theory and Its Ramifications* 21.05 (2012), p. 1250041 ([↑ 1](#)).
- [BBK21] Sebastian Baader, Ryan Blair, and Alexandra Kjuchukova. “Coxeter groups and meridional rank of links.” In: *Mathematische Annalen* 379 (2021), pp. 1533–1551 ([↑ 1, 15, 24](#)).
- [Bla+20a] Ryan Blair, Marion Campisi, Scott A Taylor, and Maggy Tomova. “Distortion and the bridge distance of knots.” In: *Journal of Topology* 13.2 (2020), pp. 669–682 ([↑ 1](#)).
- [BKM24] Ryan Blair, Alexandra Kjuchukova, and Nathaniel Morrison. “Coxeter quotients of knot groups through 16 crossings.” In: *Experimental Mathematics* (2024), pp. 1–10 ([↑ 23](#)).
- [Bla+20b] Ryan Blair, Alexandra Kjuchukova, Roman Velazquez, and Paul Villanueva. “Wirtinger systems of generators of knot groups.” In: *Communications in Analysis and Geometry* 28.2 (2020), pp. 243–262 ([↑ 1, 2, 16](#)).
- [CEH08] Toen Castle, Myfanwy E Evans, and ST Hyde. “Ravels: knot-free but not free. Novel entanglements of graphs in 3-space.” In: *New Journal of Chemistry* 32.9 (2008), pp. 1484–1492 ([↑ 1](#)).

- [CSV16] W Edwin Clark, Masahico Saito, and Leandro Vendramin. “Quandle coloring and cocycle invariants of composite knots and abelian extensions.” In: *Journal of Knot Theory and Its Ramifications* 25.05 (2016), p. 1650024 (↑ 14).
- [Cul+24] Marc Culler, Nathan M. Dunfield, Matthias Goerner, and Jeffrey R. Weeks. *SnapPy, a computer program for studying the geometry and topology of 3-manifolds*. Available at <http://snappy.computop.org>. Oct. 2024 (↑ 17).
- [FT10] Anna Felikson and Pavel Tumarkin. “Reflection subgroups of Coxeter groups.” In: *Transactions of the American Mathematical Society* 362.2 (2010), pp. 847–858 (↑ 15).
- [FM07] Thomas Fleming and Blake Mellor. “Virtual Spatial Graphs.” In: *Kobe Journal of Mathematics* 24 (2007), pp. 67–85 (↑ 12).
- [FM09] Thomas Fleming and Blake Mellor. “Counting links in complete graphs.” In: *Osaka Journal of Mathematics* 46.1 (2009), pp. 173–201 (↑ 1).
- [FT24] Konomi Furuki and Hiroshi Tamaru. “Homogeneous quandles with abelian inner automorphism groups and vertex-transitive graphs.” In: *International Electronic Journal of Geometry* 17.1 (2024), pp. 184–198 (↑ 19).
- [God97] Hiroshi Goda. “Bridge index for theta curves in the 3-sphere.” In: *Topology and its Applications* 79.3 (1997), pp. 177–196 (↑ 5).
- [GY12] Robert Gulliver and Sumio Yamada. “Total curvature of graphs after Milnor and Euler.” In: *Pacific Journal of Mathematics* 256.2 (2012), pp. 317–357 (↑ 1).
- [Har91] Masao Hara. “Symmetry of  $\theta_4$ -Curves.” In: *Tokyo Journal of Mathematics* 14.1 (1991), pp. 7–16 (↑ 18).
- [Jan+16] Byoungwook Jang, Anna Kronaueur, Pratap Luitel, Daniel Medici, Scott Taylor, and Alexander Zupan. “New examples of Brunnian theta graphs.” In: *Involve, a Journal of Mathematics* 9.5 (2016), pp. 857–875 (↑ 18–20).
- [JP24] Jason Joseph and Puttipong Pongtanapaisan. “Meridional rank and bridge number of knotted 2-spheres.” In: *Canadian Journal of Mathematics* (2024), pp. 1–18 (↑ 15).
- [Kin58] Shin’ichi Kinoshita. “Alexander polynomials as isotopy invariants. I.” In: *Osaka Journal of Mathematics* 10 (1958), pp. 263–271 (↑ 16, 18, 20).
- [Kin72] Shin’ichi Kinoshita. “On elementary ideals of polyhedra in the 3-sphere.” In: *Pacific Journal of Mathematics* 42.1 (1972), pp. 89–98 (↑ 16, 18, 20).
- [Kir97] Rob Kirby. “Problems in low-dimensional topology.” In: *Proceedings of the 1993 Georgia International Topology Conference, Geometric Topology* 2 (1997) (↑ 1).
- [LPV24] Ricky Lee, Puttipong Pongtanapaisan, and Hanh Vo. “Widths of links via diagram colorings.” In: *arXiv preprint arXiv:2401.17193* (2024) (↑ 16).
- [Liv95] Charles Livingston. “Knotted symmetric graphs.” In: *Proceedings of the American Mathematical Society* 123.3 (1995), pp. 963–967 (↑ 15).
- [Mil50] John W Milnor. “On the total curvature of knots.” In: *Annals of Mathematics* 52.2 (1950), pp. 248–257 (↑ 1).

- [Mot00] Tomoe Motohashi. “2-bridge  $\theta$ -curves in  $S^3$ .” In: *Topology and its Applications* 108.3 (2000), pp. 267–276 (↑ [1](#), [5](#)).
- [NPV24] Thieu Nguyen, Puttipong Pongtanapaisan, and Hanh Vo. “Learning bridge numbers of knots.” In: *arXiv preprint arXiv:2405.05272* (2024) (↑ [12](#)).
- [Nie10] Maciej Niebrzydowski. “Coloring invariants of spatial graphs.” In: *Journal of Knot Theory and Its Ramifications* 19.06 (2010), pp. 829–841 (↑ [12](#), [13](#)).
- [Par11] John Pardon. “On the distortion of knots on embedded surfaces.” In: *Annals of Mathematics* (2011), pp. 637–646 (↑ [1](#)).
- [Sch54] Horst Schubert. “Über eine numerische Knoteninvariante.” In: *Mathematische Zeitschrift* 61.1 (1954), pp. 245–288 (↑ [1](#)).
- [Sch56] Horst Schubert. “Knoten mit zwei Brücken.” In: *Mathematische Zeitschrift* 65.1 (1956), pp. 133–170 (↑ [1](#)).
- [SW90] Jonathan K. Simon and Keith Wolcott. “Minimally knotted graphs in  $S^3$ .” In: *Topology and its Applications* 37.2 (1990), pp. 163–180 (↑ [19](#)).
- [ST02] Teruhiko Soma and Takashi Tsuno. “Curvature index for spatial theta-curves.” In: *Differential Geometry and its Applications* 16.1 (2002), pp. 35–47 (↑ [1](#)).
- [Suz84] Shin’ichi Suzuki. “Almost unknotted-curves in the 3-sphere.” In: *Kobe journal of mathematics* 1 (1984), pp. 19–22 (↑ [19](#)).
- [TT13] Scott A Taylor and Maggy Tomova. “C-essential surfaces in (3-manifold, graph) pairs.” In: *Communications in Analysis and Geometry* 21.2 (2013), pp. 295–330 (↑ [4](#)).
- [TT21] Scott A Taylor and Maggy Tomova. “Tunnel number and bridge number of composite genus 2 spatial graphs.” In: *Pacific Journal of Mathematics* 314.2 (2021), pp. 451–494 (↑ [1](#)).
- [Tsu03] Takashi Tsuno. “Bridge index for spatial  $\theta_n$ -curves with local knots.” In: *Topology and its Applications* 129.2 (2003), pp. 159–176 (↑ [5](#)).
- [Wol87] Keith Wolcott. “The knotting of theta curves and other graphs in  $S^3$ .” In: *Geometry and Topology: Manifolds, Varieties, and Knots (Athens, GA, 1985)*. Vol. 105. Lecture Notes in Pure and Applied Mathematics. Dekker, New York, 1987, pp. 325–346 (↑ [18](#), [20](#)).

Sarah Blackwell  
 University of Virginia  
 Email address: [blackwell@virginia.edu](mailto:blackwell@virginia.edu)  
 URL: <https://seblackwell.com/>

Puttipong Pongtanapaisan  
 Arizona State University  
 Email address: [ppongatan@asu.edu](mailto:ppongatan@asu.edu)  
 URL: <https://puttipongtanapaisan.wordpress.com/>

Hanh Vo  
Arizona State University  
Email address: [thihanhv@asu.edu](mailto:thihanhv@asu.edu)  
URL: <https://hanhv.github.io/>